Article

JOURNAL OF THE CHINESE CHEMICAL SOCIETY

Inulin Hydrolysis by Immobilized Inulinase on Functionalized Magnetic Nanoparticles Using Soy Protein Isolate and Bovine Serum Albumin

Homa Torabizadeh,[a]* Mohaddeseh Mikani[b] and Reza Rahmanian[c]

[a]*Department of Chemical Technologies, Iranian Research Organization for Science and Technology (IROST), P.O. Box 33535111, Tehran, 33853, Iran*
[b]*Department of Agriculture, Iranian Research Organization for Science and Technology (IROST), Tehran, 33853, Iran*
[c]*Young Researchers and Elite Club, North Tehran Branch, Islamic Azad University, Tehran, 32454, Iran*

(Received: October 14, 2017; Accepted: December 31, 2017; Published Online: February 2, 2018; DOI: 10.1002/jccs.201700364)

Inulin hydrolysis was performed by inulinase from *Aspergillus niger* covalently immobilized on magnetite nanoparticles (Fe_3O_4) covered with soy protein isolate (Fe_3O_4/SPI) functionalized by bovine serum albumin (Fe_3O_4/SPI/BSA) nanoparticles as a new bio-functional carrier. The specific activity and protein content of the immobilized enzyme were 25.99 U/mg and 3.52 mg/mL, respectively, with 80% enzyme loading. The immobilized inulinase showed maximum activity at 45 °C, which is 5 °C higher than the optimum temperature of the free enzyme. Also, the optimum pH of the immobilized enzyme shifted from 6 to 5.5, which is more acidic compared to that of the free enzyme. The K_m value of immobilized inulinase decreased to 2.03 mg/mL. Thermal stability increased considerably at 65 and 75 °C, and a 5.13-fold rise was detected in the enzyme half-life at 75 °C after immobilization. Moreover, 80% of initial activity of immobilized inulinase remained after 10 cycles of hydrolysis.

Keywords: Functionalized magnetic nanoparticle; Inulin; Inulinase immobilization; Soy protein isolate and bovine serum albumin; Fructose and Fructooligosaccharide.

INTRODUCTION

Fructose and fructooligosaccharides (FOSs) are important and fast emerging components in food, beverages, and pharmaceutical products. One of the most important health benefits of fructose as a sweetener is its insulin-independent metabolism, which makes it a sugar for diabetic patients. It has low carcinogenicity, raises iron absorption and zinc in children, and enhances the flavor, color, and product stability in food and beverages.[1–5] Fructose in crystalline form is about 1.8 and 2.3 times sweeter than the table sugar sucrose and glucose, respectively.[4] Inulin is a polysaccharide consisting of linear b-2,1 linked polyfructose units, which are responsible for its nutritional characteristics and are known to be perfect sources of fructose and high fructose syrup (HFS).[6,7] FOSs are nondigestible carbohydrates that reach the large intestine, where colonic flora ferment them by enhancing the bifidobacteria growth and prevent the growth of pathogenic microorganisms.[8,9] From a physiological point of view, FOSs behave as a soluble food fiber. They have remarkable characteristics. For example, they are calorie-free, which means that human body lacks the essential enzymes to hydrolyze the β-bonds and so that the digestive enzymes cannot hydrolyze them. Thus, since these substances cannot be used as an energy source in the body, they are safe for diabetics and people on slimming diets.[10,11] Another important characteristic of FOSs is that they have a low sweetness intensity. This property makes them suitable for numerous kinds of foods where the sucrose use is restricted because of its high sweetness.[11] FOSs have prebiotic effect. It is usually accepted that the bacterial community *residing* in the human gastrointestinal tract has a vital impact on intestinal functioning and human health.[12] These properties, together with their other favorable physiological effects (increased mineral absorption, low carcinogenicity, and reduced levels of serum cholesterol, phospholipid, and triacylglycerol), support FOS addition

*Corresponding author. Email: htoraby@alumni.ut.ac.ir

 © 2018 The Chemical Society Located in Taipei & Wiley-VCH Verlag GmbH & Co. KGaA, Weinheim

to foods.[10,11] Inulin is a stored carbohydrate in the roots of Jerusalem artichoke, chicory, and tubers, and can be used in industrial scales to produce HFS.[13]

Fructose can be obtained by the hydrolysis of starch by enzymes including α-amylase, amyloglucosidase, pullulanase, and glucose isomerase, resulting in the production of a mixture of oligosaccharides (8%), fructose (45%), and glucose (50%). Separation of fructose from this HFS is expensive and thus makes this process wasteful. An alternative method involves the use of inulinase, which yields 95% pure fructose after single stage of enzymatic hydrolysis of inulin.[14–16]

Inulinase is one of the most important enzymes with industrial application. This enzyme is a β-fructanohydrolase (endo-inulinase, EC 3.2.1.7 and exo-inulinase EC 3.2.1.80) that produces fructose and FOSs by the degradation of inulin (Scheme 1).[17,18]

Enzyme immobilization appears to be a key factor in developing thermal stability, reutilization, and reusability of the enzyme. Immobilized enzymes have to maintain their structure and function to retain their biological activity after immobilization, to remain tightly bound to the surface, and not to be desorbed during their use. Immobilization removes most of the disadvantages of the enzyme applications, making their use promising in industrial processes.[19,20]

Enzyme immobilization by a technique based on the formation of covalent bonds is a widely used application of inulinase. An advantage of this method is that, because of the stable nature of the bonds formed between the enzyme and the carrier, the enzyme is not released into the solution upon its use.[21,22]

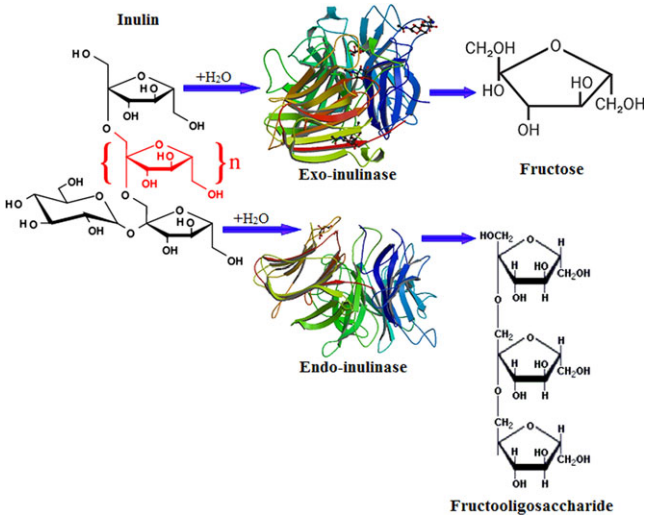

Scheme 1. Schematic representation of inulin hydrolysis by endo and exo-inulinase.

Magnetic nanoparticles have been subjects of intense research because of their excellent physical and chemical characteristics such as superparamagnetism, good dispersity, low toxicity, and good biocompatibility. Moreover, bare iron magnetic nanoparticles have hydrophobic surfaces. Owing to the hydrophobic interactions between the nanoparticles, these particles are unstable and tend to aggregate. Thus, the particle size increases and their magnetic properties can change in complex environmental and natural systems. Various modification methods have been suggested to get biocompatible and soluble magnetic iron. Nanoparticles for inulinase immobilization covered with soy protein isolate (SPI) (to prevent Fe_3O_4 aggregation) accomplished by bovine serum albumin (BSA) (as a source of lysine group linker to enhance inulinase covalent binding) proteins (Fe_3O_4/SPI/BSA) are considered to be one of the most promising materials as protective layers of magnetic nanoparticles owing to their higher biocompatibility and hydrophilic property. Thus, they are typically applied to fabricate magnetic protein nanoparticles suitable for inulinase immobilization. These nanoscaled systems showed several advantages such as increased surface area and reactivity and enhanced enzyme loading capacity (ELC).[23–27] In the present study, we aim to further improve and enhance the ELC, thermal stability, and reusability of the immobilized enzyme.

EXPERIMENTAL

Materials

Inulin from chicory roots was obtained from Fluka Chemical Company (Switzerland). Inulinase (endo-inulinase EC 3.2.1.7 and exo-inulinase EC 3.2.1.80) from Aspergillus niger was obtained from Sigma-Aldrich. Glutaraldehyde (25% v/v in water), sodium potassium tartrate, and BSA were purchased from Merck. All other solvents and reagents used were of analytical grade and purchased from Merck and Sigma-Aldrich

Surface analysis was carried out using a Tescan Mira II (USA) field-emission scanning electron microscope (FE-SEM) at a voltage of 20.0 kV after coating the samples with a thin layer of gold by magnetron sputtering. For measuring the absorbance, a Perkin

 © 2018 The Chemical Society Located in Taipei & Wiley-VCH Verlag GmbH & Co. KGaA, Weinheim

Elmer Lambda 25 UV–vis spectrophotometer (USA) was used employing cells of 1-cm path length against blanks. The infrared spectra of all formulations were recorded using a Fourier transform infrared spectrometer (FTIR-8300, Shimadzu, Japan). All values are expressed as mean ± standard deviation of three replicate experiments.

Nanomagnetite preparation

Magnetic nanoparticles were synthesized by coprecipitation of magnetic nanoparticles. A mixed solution of ferric and ferrous ions in 1:2 molar ratio was prepared. First, 8.86 g $FeCl_3 \cdot 6H_2O$ (99% purity) and 3.25 g $FeCl_2 \cdot 4H_2O$ (99% purity) were dissolved in 400 mL of deionized water in a three-necked flask under nitrogen atmosphere. Then, 10 mL sodium hydroxide solution was added dropwise into the flask under constant stirring. After mixing the solution, its color changed from light brown to black, indicating the formation of Fe_3O_4 nanoparticles. Ultrasonication at 200 Hz frequency was applied for 10 min at room temperature for size reduction of the magnetic particles, which were then kept at ambient temperature overnight. The resulting Fe_3O_4 nanoparticles were separated by an external magnetic field and then washed with water three times. Finally, the magnetic Fe_3O_4 nanoparticles were dispersed in deionized water.[28–31] The reaction principle is as follows:

$$2Fe_3 + + Fe_2 + + 8OH - \cdot Fe_3O_4 + 4H_2O \qquad (1)$$

SPI/BSA nanostructure preparation

The desolvation technique was employed for the preparation of SPI nanostructure covered with BSA. For this, a mixed solution of SPI and BSA in 8:1 molar ratio was prepared, and the pH was adjusted to 9 by NaOH solution (0.1 M) with stirring. Then ultrasonication was carried out to make a homogeneous solution. The nanostructure was formed by the dropwise addition of the desolvating agent to the solution under constant stirring until the solution became turbid. After the desolvation process, the desolvating agent was evaporated using a Buchi Rotavapor R114 at 30°C and was replaced with the same volume of deionized water.[23,25,32]

Synthesis of Fe_3O_4/SPI/BSA nanostructure

First, an appropriate amount of SPI/BSA nanoparticles was dissolved in 25 mL phosphate buffered saline (PBS). Some amount of Fe_3O_4 magnetic nanoparticles was added to the SPI-BSA solution. Next, glutaraldehyde was added to deposit the SPI-BSA on Fe_3O_4 nanoparticles with cross-linking. The cross-linking process was implemented under stirring of the suspension over 3 h. The resulting Fe_3O_4/SPI/BSA nanoparticles were separated using centrifugal separation at 13 000 rpm and washed with deionized water to remove the unreacted SPI-BSA as much as possible.[27,28]

Inulinase immobilization on Fe_3O_4/SPI/BSA nanostructure

Covalent immobilization was performed by mixing the Fe_3O_4/SPI/BSA nanostructure and the enzyme solution and stirring for 24 h at 4 °C. For covalent attachment, glutaraldehyde (25 mg/mL aqueous solution) in 50 mM sodium acetate buffer at pH 5.4 was used as the cross-linking agent. Eventually, for removing trapped, nonbound enzyme, the products obtained were isolated using centrifugal separation and washed three times with 50 mM sodium acetate buffer solution to remove the free enzyme.[13,33,34]

Scanning electron microscopy

SEM examination of Fe_3O_4/SPI/BSA/inulinase nanostructure was carried out with the MIRA/TESCAN microscope. A sample was lyophilized and then placed on carbon tape over a microscope slide to be coated with gold under vacuum to record the SEM images. Representative micrographs were obtained for each sample at magnifications of ×500 and ×1500.

Enzyme loading

The mass ratio of immobilized inulinase on the nanoparticles shows the ELC. Moreover, ELC of inulinase can be identified as the enzyme units loaded per gram of the supporting agents.[14,35]

Nanoparticles provide large surface area per unit mass for high enzyme loading. The ELC of enzyme units per gram of the supporting agents was estimated using Eq. (2):

$$Q = \frac{(C_1 - C_2)V}{W} \qquad (2)$$

where Q is the value of enzyme loading (mg per mg support), C_1 is the concentration of protein in the inulinase solution before immobilization, C_2 is the protein concentration of the residual free enzyme in the cocktail after immobilization, V is the total solution volume, and W is the weight of carrier [mg]. The protein content of inulinase was determined using Bradford's method.[14,35,36]

Determination of inulinase activity and protein content

The activity of free and immobilized inulinase was estimated by measuring the amount of reducing sugars released from inulin using the 3,5-dinitrosalicylic acid (DNS) method. The nanostructure loaded with native or immobilized inulinase was incubated with 9000 μL of 50 mM sodium acetate buffer at pH 5.5 containing 900 μL of 1 M inulin. The assay mixture for inulinase activity was hydrolyzed for 60 min in a water bath at 40°C. Then, the reaction was stopped by adding 500 μL of the DNS reagent to 500 μL of the hydrolyzed mixture and incubating the mixture at 97–98 °C for 10 min. A separate control sample was prepared for each sample to correct the non-enzymatic release of fructose. The activity and product content of the native and immobilized inulinase were determined by reading the absorbance intensity at 575 nm using, the UV–vis spectrophotometer using cells of 1-cm path length. The absorbance was related to the concentration of fructose with a standard calibration curve. All experiments were repeated at least three times to ensure reproducibility. One unit of inulinase activity was defined as the amount of inulinase enzyme that produced 1 μmol fructose per minute under standard assay conditions:[19,34,37,38]

$$\text{Activity} = \frac{\mu\text{mol fructose}}{\text{min}} \tag{3}$$

The protein concentration of the immobilized enzyme was estimated by taking into consideration the protein concentration in the initial solution and the concentration of the unbound protein:

$$\text{Protein content} = \left(\frac{\text{Abs}}{f}\right) * 10 D_f \tag{4}$$

where unit of protein content is in milligram per milliliter; Abs is the absorbance at 595 nm, D_f denotes the dilution factor of the samples; and f is the factor obtained from the standard curve.[19,36]

Effect of temperature on the activity of free and immobilized inulinase

The effect of temperature on the activity of the free and immobilized enzyme was determined by incubating the enzyme in 0.1 M sodium acetate buffer (pH 5.5) without substrate at different temperatures ranging from 35 to 75°C for 90 min, and then determining the enzyme activity by the DNS method as described earlier. The highest enzyme activity is taken as 100% and the relative activity at each temperature is expressed as a percentage of the of the maximum (100%) activity. The inactivation rate constant of inulinase (k_{in}) [min^{-1}] was determined using Eq. (5):[35,37,38]

$$\ln A_t/A_0 = -k_{in} \times t \tag{5}$$

where A_0 is inulinase activity before incubation, A_t is inulinase activity after incubation at the temperature of interest, and t is the incubation time. The half-life of inulinase ($t_{1/2}$, min), which is the time required to reduce the activity by 50%, was estimated using Eq. (6).[13,35]

Effect of pH on the activity of free and immobilized inulinase

To determine the optimum pHs for the activities of native and immobilized enzyme, inulin solution dissolved in buffer for each enzyme was separately incubated under the various pH values in the range 3–8 (pH 3–5, 0.1 M acetate buffer; pH 6–8, phosphate buffer) at 40°C.[3,38] The highest enzyme activity is represented as 100%, and the activity at each pH is expressed relatively as a percentage of the 100% activity. Residual activity was measured in terms of relative activity.

Determination of enzyme half-life

Half-life is described as the time, in minutes, needed for the residual enzymatic activity in the sample to reach one-half of its initial value:[35,37,38]

$$t_{1/2} = \ln 2/k_d \tag{6}$$

 © 2018 The Chemical Society Located in Taipei & Wiley-VCH Verlag GmbH & Co. KGaA, Weinheim

Determination of kinetic parameters

The apparent values of K_m (substrate concentration at half the maximum velocity) and V_{max} (maximum velocity) were measured from the kinetic data by applying different inulin concentrations (0.25–5 mg mL-1) in sodium acetate buffer (0.1 M, pH 5.5) at 40 °C. The Line–Weaver–Burk plot (double reciprocal) method was used to obtain the Michaelis–Menten kinetic model to explain the hydrolysis of inulin by the native and the immobilized enzyme.[2,13,17,20]

Michaelis–Menten equation provides a good description of the enzyme kinetics when the concentration of the substrate is high. The plot provides a straightforward graphical method for analysis of the Michaelis–Menten equation, using which 1/[*S*] is plotted against 1/[*V*] (Table 1); where, V_{max} is the maximum enzyme rate and K_m is the Michaelis constant and is equal to the substrate concentration at which the reaction rate is half its maximum value.[2,13,17,20] The kinetic constants of native and immobilized inulinase were estimated using the double reciprocal plot method (Lineweaver–Burk plot).

Reusability of immobilized inulinase

Reusability of the immobilized enzyme was analyzed by incubating inulinase-loaded nanostructure with 9000 μL of 50 mM sodium acetate buffer at pH 5.5 containing 900 μL inulin and hydrolyzing the mixture for 60 min in a water bath at 40°C. The reaction was stopped by adding 500 μL of DNS reagent to 500 μL of hydrolyzed mixture and incubating the mixture at 97–98°C for 10 min and finally reading the absorbance intensity at 575 nm against the blank.

After each cycle, the enzyme-loaded nanostructures were washed with sodium acetate buffer and re-added to a fresh reaction mixture (9000 μL of 50 mM sodium acetate buffer at pH 5.5 containing 900 μL inulin) for another enzyme assay and this process was repeated for 15 cycles.[13] Relative activity was expressed as the ratio of the residual activity to the initial activity.

RESULTS AND DISCUSSION

FE-SEM analysis

The morphology and size of nanomagnetite were analyzed using FE-SEM, (Figure 1). Uniform Fe_3O_4 nanoparticle surface and the size distribution histogram are presented in Figure 1(a) and (b), respectively. The morphology and particle size distribution graph of SPI is shown in Figure 1(c) and (d). In addition, surface characterization of the uniform SPI/BSA nanostructure with size distribution histogram for SPI/BSA is presented in Figures 1 (e) and (f).

Enzyme loading

The ELC was calculated using Eq. (2). The protein content of inulinase was quantified by applying Bradford's method. The enzyme loading under the described immobilization conditions was nearly 3.55 mg enzyme/mg of support.

Determination of inulinase activity and protein content

The results of this work show that optimal activity of free inulinase results after 3 min of reaction at the temperature 35–40°C. However, in the case of the immobilized enzyme, this time is altered to 5 min (Figure 2).

The protein assays of free and immobilized enzyme were 4.477 and 3.526 (mg/mL), respectively.

Optimization of temperature, and temperature stability of immobilized inulinase

The optimum temperature of the immobilized enzyme, compared with that of the free state, shows a shift from 40 to 45°C (Figure 3); which is 5 °C higher than that of free enzyme. This shift of the enzyme's optimum temperature after immobilization could be attributed to the formation of a molecular cage around the protein molecule (enzyme), which protected the enzyme's molecules from the bulk temperature.[37,38]

The results clearly indicate that at 45°C the relative activity of the immobilized enzyme was considerably increased compared to that at the other temperatures studied (35, 55, 65, and 75°C).

The temperature effect on the stability of the free and immobilized inulinase is presented in Figure 3. These results confirm that the activity of immobilized inulinase is more robust than that of the free form against heat inactivation. At 65 °C, immobilized inulinase retained over 50% of its initial activity after the incubation period of 90 min. It is clear that the stability of the immobilized enzymes at 35 and 50 °C for an incubation period of 90 min did not change considerably, whereas that of the free enzymereduced gradually. In this regard, 60 °C is the temperature at which the enzymes are to be preferably applied in industrial processes to prevent microbial growth; and it permits

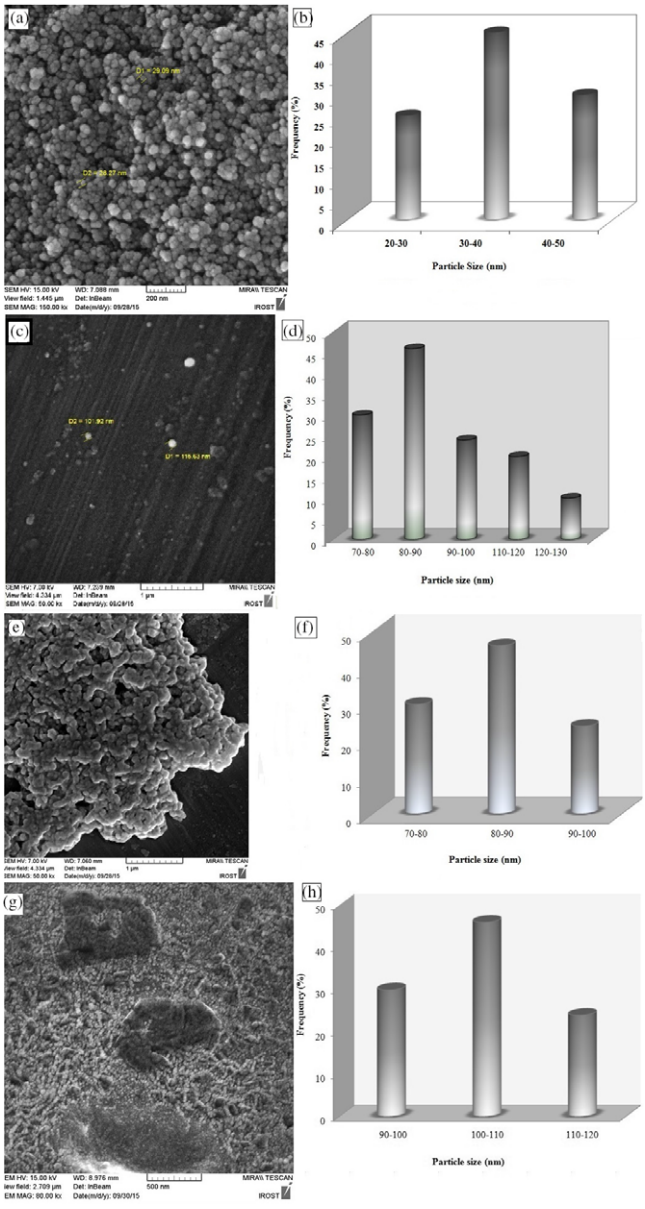

Fig. 1. SEM images and Particle size distribution graphs of nanoparticles. Magnetic nanoparticles (1a and 1b), SPI nanoparticles (1c and 1d), SPI-BSA nanoparticles (1e and 1f), Fe_3O_4@SPI-BSA NPs (1g and 1h).

higher concentration of the sugars, an ideal condition for inulinase to produce fructose and FOS.[37,38]

At 65°C, free enzyme activity decreased to 17%, whereas that of the immobilized enzyme retained 54% of its initial activity. These results are very encouraging for industrial applications. However, the thermal stability of the immobilized inulinase was significantly increased compared to that of free enzyme. That is, the native inulinase was very

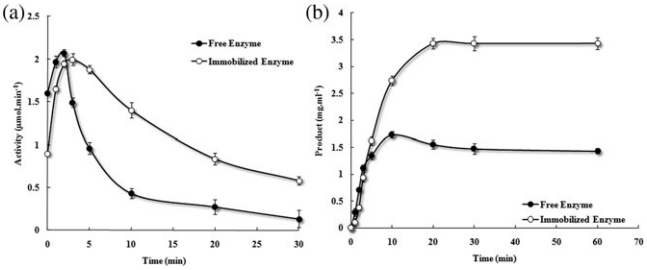

Fig. 2. Enzyme activity and hydrolysis profile of free and immobilized inulinase. Comparison of enzyme activity of free and immobilized inulinase (a), and hydrolysis profile of free and immobilized inulinase (b).

unstable at temperatures in excess of 55 °C, while the immobilized enzyme was moderately stable up to 65 °C. Enzyme hydrolysis of inulin at high temperature was effective in improving the solubility of the substrate and accelerating reaction rate. The enzyme molecule's covalent attachment to carriers at multiple points increased the rigidity of the enzyme structure and it was difficult to denature it when heated, thus it could retain its stable structure and improve its thermal stability. The covalent linkages between the enzyme and carrier protected the structure of the active site from deformation by heat.[13,20,35,37,38]

Effect of pH on the activity of free and immobilized inulinase

A lower optimum pH is useful for the preparation of HFS because it avoids unwanted color formation.[3,38] The highest activity of inulinase was observed at pH 6.0, whereas the optimum pH of the immobilized enzyme was shifted. As shown in Figure 4, this shift occurs in the direction of acidic pH (=5.5), probably because of the difference in micro environment such as the surface charge of the carrier material.[38] As shown in Figure 5, free and immobilized enzymes were quite stable in the pH range 4.5–7.5, and the pH stability was basically enhanced after immobilization.

However, broader curves were observed for both temperature–activity and the pH–activity profiles when the immobilized forms were compared with the free form. Such a feature may be ascribed to a protective microenvironment resulting of immobilization, which renders the enzyme less sensitive to the operational conditions in the bulk phase.

 © 2018 The Chemical Society Located in Taipei & Wiley-VCH Verlag GmbH & Co. KGaA, Weinheim

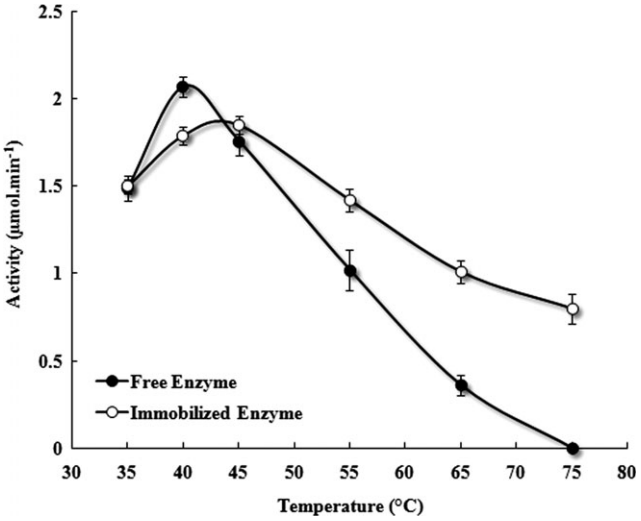

Fig. 3. Effect of temperature on enzyme activity.

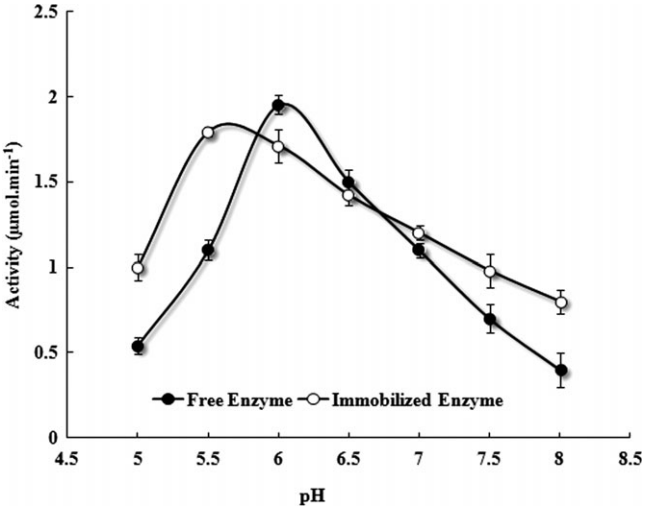

Fig. 4. Effect of pH on enzyme activity.

Half-life of the enzymes

Half-lives of the enzymes were determined by Eq. (5), and an improvement in the half-life of the immobilized enzyme was obtained compared to that of the free enzyme. Obviously, the $t_{1/2}$ values were reduced by increasing the incubation temperature.[13,35] However, the $t_{1/2}$ values of immobilized enzyme increased by 6.46- and 5.13-fold at 65and 75 °C, respectively, which are significantly higher than those of the free enzyme at the chosen incubation temperatures. The immobilized inulinase was thus more stable than the free enzyme (Table 1).

Kinetic studies

The kinetic constants of the native and immobilized inulinase were estimated using the double-reciprocal plot method (Lineweaver–Burk plots). The obtained values are shown in Table 2.

The V_{max} and K_m of free inulinase were 0.829 μmol/min and 2.72 mg/mL, respectively. For the immobilized enzyme, V_{max} and K_m were 0.674 μmol/min and 2.03 mg/mL, respectively. After immobilization, the apparent K_m decreased, indicating that a lower concentration of the substrate is needed for the immobilized enzyme since the immobilized enzymes are as accessible as the free enzymes to the substrates. It shows that immobilization decreases the diffusion and permeation rates of the substrate and the product. The lower Km value of the immobilized inulinase for inulin makes it a better candidate for inulin hydrolysis. Such a small reduction in both K_m and V_{max} values after immobilization is not unusual. Immobilization did not considerably affect V_{max} of the free enzyme. It could be due to changes in effective localized charges near the active site of the enzyme, because the enzyme attaches to the support very tightly. Also, after immobilization, the mass transfer limitsthe substrate accessibility to the active site of the enzyme.

Table 1. Half-life of the free and immobilized inulinase at three different temperatures

	Half-life (min)		
	55°C	65°C	75°C
Free enzyme	182	63	30
Immobilized enzyme	495	407	154

Reusability study

The immobilized biocatalyst was used repeatedly in several batch hydrolysis runs. The main advantage of immobilization of enzyme is the easy separation and reusability.[13] The data in Figure 5 reveal that the immobilized inulinase retained over 80% of its activity after 10 cycles (Figure 5).

Hence, the immobilized inulinase on the nanomagnetite could be reused for more number of times and retain more enzyme activity than the native enzyme, thereby, it saving substantial cost, time, carriers, and enzymes. The most important consideration of immobilized enzymes for industrial application is their repeated use.[13,37] It was

Table 2. Michaelis–Menten constant (K_m) and V_{max} of free and immobilized enzyme

	K_m (mg/mL)	V_{max} (μmol/min)
Free enzyme	2.72	0.829
Immobilized enzyme	2.03	0.674

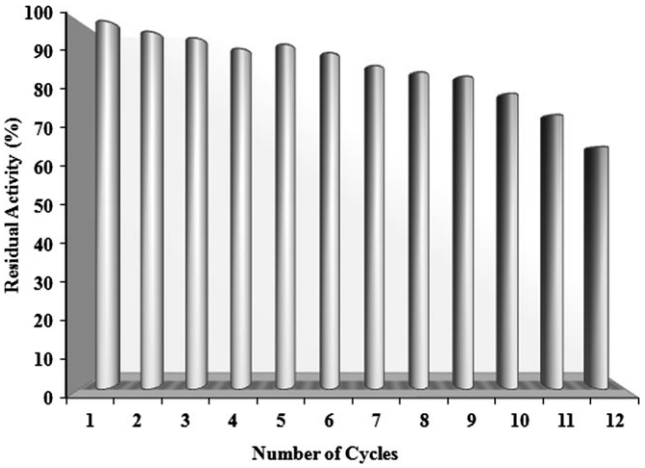

Fig. 5. Effect of the enzyme reuse on the activity of immobilized inulinase during inulin hydrolysis at pH 5.5 and 40°C for 60 min. Each treatment was performed in triplicate.

observed that up to four cycles there was no significant loss in activity, but it started to reduce thereafter.

CONCLUSIONS

Application of functionalized magnetic nanoparticles to immobilize inulinase for inulin hydrolysis was studied in the present work. Successful immobilization was confirmed using FE-SEM and enzyme assays. This study is the first in which Fe_3O_4/SPI/BSA is used as a carrier for inulinase immobilization. The relative activity of the immobilized enzyme was significantly higher than that of the free enzyme at 50–70 °C. The thermal stability of the enzyme improved by immobilization. The immobilized enzyme showed an increase in pH stability over the studied pH range of 5–8. The kinetic parameters were effective in both free and immobilized forms of inulinase. Our results showed that the enzyme molecules often undergo conformational changes during immobilization, resulting in a change in the temperature stability, and kinetic constants. The study of reusability of immobilized inulinase showed that even after 10 cycles the enzyme retained 80% of its initial activity. Overall, this immobilized system provides numerous advantages for the industrial production of HFS.

ACKNOWLEDGMENTS

The financial support provided by Iranian Research Organization for Science and Technology (IROST) and Iran Nanotechnology Initiative Council (INIC) is greatly acknowledged.

REFERENCES

1. L. M. Hanover, J. S. White, *Am. J. Clin. Nutr.* **1993**, *58*, 724.
2. P. K. Gill, R. K. Manhas, P. J. Singh, *J. Food Eng.* **2006**, *76*, 369.
3. T. Yewale, R. S. Singhal, A. A. Vaidya, *Biocatal. Agric. Biotechnol.* **2013**, *2*, 96.
4. T. M. Mohamed, S. M. El-Souod, E. M. Ali, M. O. El-Badry, M. M. El-Keiy, *J. Biosci.* **2014**, *39*, 785.
5. C. Altunbas, M. Uygun, D. Uygun, S. Akgöl, A. Denizli, *Appl. Biochem. Biotechnol.* **2013**, *170*, 1909.
6. N. Kaur, A. Gupt, *J. Biosci.* **2002**, *27*, 703.
7. E. Ricca, V. Calabro, S. Curcio, G. Iorio, *Process Biochem.* **2009**, *44*, 466.
8. F. R. Bornet, F. Brouns, Y. Tashiro, V. Duvillier, *Dig. Liver Dis.* **2002**, *34*, 111.
9. G. Kelly, *Altern. Med. Rev.* **2009**, *13*, 315.
10. M. Rivero-Urgell, A. Santamaria-Orleans, *Early Hum. Dev.* **2001**, *65*, 43.
11. J. W. Yun, *Enzyme Microb. Technol.* **1996**, *19*, 107.
12. M. Blaut, *Eur. J. Nutr.* **2002**, *41*, 11.
13. Q. D. Nguyen, J. M. Rezessy, B. Czukor, A. Hoschke, *Process Biochem.* **2011**, *46*, 298.
14. M. M. Elnashar, E. N. Danial, G. E. Awad, *Ind. Eng. Chem. Res.* **2009**, *48*, 9781.
15. C. H. Kim, S. K. Rhee, *Biotechnol. Lett.* **1989**, *11*, 201.
16. T. Nakamura, Y. Ogata, S. Akichika, A. Nakamura, K. Ohta, *J. Ferment. Bioeng.* **1995**, *80*, 164.
17. E. N. Danial, M. M. Elnashar, G. E. Awad, *Ind. Eng. Chem. Res.* **2009**, *49*, 3120.
18. D. Derycke, E. J. Vandamme, *J. Chem. Technol. Biotechnol.* **1984**, *34*, 45.
19. A. Richetti, C. B. Munaretto, L. A. Lerin, L. Batistella, J. V. Oliveira, R. M. Dallago, V. Astolfi, *Bioprocess Biosyst. Eng.* **2011**, *35*, 383.
20. R. S. Singh, R. P. Singh, J. F. Kennedy, *Int. J. Biol. Macromolec.* **2017**, *95*, 87.
21. S. Datta, L. R. Christena, Y. Rani, S. Rajaram, *3Biotech* **2012**, *3*, 1.
22. I. V. Shkutina, O. F. Stoyanova, V. F. Selemenev, *Russ. J. Bioorg. Chem.* **2017**, *42*, 748.

 © 2018 The Chemical Society Located in Taipei & Wiley-VCH Verlag GmbH & Co. KGaA, Weinheim

23. J. Y. Jun, H. H. Nguyen, S. Y. R. Paik, H. S. Chun, B. C. Kang, S. Ko, *Food Chem.* **2011**, *127*, 1892.
24. W. Lohcharoenkal, L. Wang, Y. C. Chen, Y. Rojanasakul, *Biomed. Res. Int.* **2014**, *2014*, 1.
25. Z. Teng, Y. Luo, Q. Wang, *J. Agric. Food Chem.* **2012**, *60*, 2712.
26. J. Xu, C. Ju, J. Sheng, F. Wang, Q. G. Zhang, M. Sun, *Bull. Korean Chem. Soc.* **2013**, *34*, 11465.
27. L. Zhanfeng, Q. Linhui, Z. Shuangling, W. Hongyan, C. Xuejun, *Eng. Asp.* **2013**, *436*, 1145.
28. A. Javid, S. Ahmadian, A. A. Saboury, S. M. Kalantar, S. Rezaei-Zarchi, *Chem. Biol. Drug Des.* **2013**, *82*, 296.
29. N. D. Kandpal, S. Sah, R. Loshali, R. Joshi, J. Prasad, *J. Sci. Ind. Res.* **2014**, *73*, 87.
30. M. C. Mascolo, Y. Pei, T. A. Ring, *Materials* **2013**, *6*, 5549.
31. Y. Weia, B. Hanb, X. Hua, Y. Linc, X. Wangd, X. Denga, *Procedia. Eng.* **2012**, *27*, 632.
32. M. Sadeghi, F. Shafiei, E. Mohammadinasab, M. J. Khodabakhshi, L. Mansouri, *Int. J. Biosci.* **2014**, *4*, 185.
33. Y. Gao, I. Kyratzis, *Bioconjug. Chem.* **2008**, *19*, 1945.
34. J. Missau, A. J. Scheid, E. L. Foletto, S. L. Jahn, M. A. Mazutti, R. C. Kuhn, *Sustain. Chem. Process.* **2014**, *2*, 2.
35. E. A. Ghada, R. Hala, A. A. Wehaid, E. H. Mohamed, *Colloid Polym. Sci.* **2017**, *295*, 495.
36. M. M. Bradford, *Anal. Biochem.* **1976**, *72*, 248.
37. R. Catana, B. S. Ferreira, J. M. Cabral, P. Fernandes, *Food Chem.* **2005**, *91*, 517.
38. A. M. P. Santos, M. G. Oliveira, F. Maugeri, *Bioresour. Technol.* **2007**, *98*, 3142.

 © 2018 The Chemical Society Located in Taipei & Wiley-VCH Verlag GmbH & Co. KGaA, Weinheim